

Electronic Supplementary Information

Conjugated Macro-Microporous Polymer Films Bearing Tetraphenylethylenes for the Enhanced Sensing of Nitrotoluenes

Chang Wan Kang,^{†,‡} Doo Hun Lee,^{†,‡} Young Jun Shin,[†] Jaewon Choi,[○] Yoon-Joo Ko,[∞]
Sang Moon Lee,[§] Hae Jin Kim,[§] Kyoung Chul Ko,^{Δ*} and Seung Uk Son^{†,*}

[†] Department of Chemistry, Sungkyunkwan University, Suwon 16419, Korea

[○] Jeonbuk Institute of Advanced Composite Materials, Korea Institute of Science and Technology, Jeonbuk-do 55324, Korea

[∞] Laboratory of Nuclear Magnetic Resonance, National Center for Inter-University Research Facilities (NCIRF),
Seoul National University, Seoul 08826, Korea

[§] Korea Basic Science Institute, Daejeon 34133, Korea

^Δ Department of Chemistry Education, Chonnam National University, Gwangju 61186, Korea

E-mail address of corresponding author: sson@skku.edu, kcho1982@jnu.ac.kr

Experimental Sections

Scanning electron microscopy (SEM) and transmission electron microscopy (TEM) images were obtained using a JSM6700F and a JEOL 2100F, respectively. Powder X-ray diffraction (PXRD) patterns were obtained using a Rigaku MAX-2200. The surface areas were obtained through the analysis of N₂ adsorption-desorption isotherm curves obtained at 77K using a Micromeritics ASAP2020. Pore size distribution was analyzed by the density functional theory (DFT) method. Thermogravimetric analysis (TGA) was conducted using under N₂ using a Seiko Exstar 7300. Infrared absorption spectra were obtained using a Bruker VERTEX 70 FT-IR spectrometer. UV/visible absorption spectra were obtained through diffuse reflectance spectroscopy using a SHIMADZU UN-3600. The emission spectra were obtained using a JASCO FP-6200. Solid state ¹³C nuclear magnetic resonance spectroscopy (NMR) was conducted at CP-TOSS mode using a 500 MHz Bruker ADVANCE II NMR equipment at the NCIRF of Seoul National University. A 4 mm magic angle spinning probe was used with a spinning rate of 5 kHz.

Synthetic procedure for MA-CMP-F and control CMP-F

Silica spheres with an average diameter of 400 nm were prepared by the Stöber method.¹ In our work, the synthetic procedures were as follows. Ethanol (200 mL), water (23.5 mL), and ammonia solution (28-30%, 7 mL) were added to a 250 mL round bottomed flask. The solution was stirred at 600 rpm for 10 min. After tetraethylorthosilicate (TEOS, 17.5 mL, 74.2 mmol) was added to solution, the mixture was stirred with 600 rpm at room temperature for 18 h. The silica spheres were retrieved by centrifugation, washed with a 1:1 mixture of methanol and ethanol three times, and dried under vacuum. A slide glass plate (7.5 cm × 2.5 cm × 0.1 cm, Paul Marienfeld GmbH & Co.) was washed through sonication for 1 h in a mixture of 37% HCl (50 mL) and water (450 mL) in a 500 mL beaker. After the glass plate was washed with distilled water until the neutralization was confirmed, it was dried using N₂ flush. Silica spheres (0.30 g) were added to ethanol (60 mL) in a 70 mL vial and sonicated for 6 h. After the glass plate was added to the vial containing silica spheres, the

setting was added to oven at 50°C. After 4 days, the assembled silica spheres on the glass plate were obtained.

1,1,2,2-Tetra(4-bromophenyl)ethane and 1,1,2,2-tetra(4-ethynylphenyl)ethane were prepared by the synthetic procedures in the literature.² The glass plate with assembled silica spheres (the plate was cut to the size of 6 cm × 2.5 cm) was added to a Rodaviss glassware (100 mL). After (PPh₃)₂PdCl₂ (3.4 mg, 4.8 μmol), CuI (0.9 mg, 4.8 μmol), triethylamine (TEA, 30 mL), and toluene (20 mL) were added to the Rodaviss glassware, the mixture was stirred at 600 rpm for 1 h. The 1,1,2,2-tetra(4-bromophenyl)ethane (31 mg, 48 μmol) and 1,1,2,2-tetra(4-ethynylphenyl)ethane (21 mg, 48 μmol) were dissolved in toluene (3 mL). After the solution was added to the Rodaviss glassware, the mixture was stirred at 600 rpm for 10 min and heated at 80°C overnight *without stirring*. After being cooled to room temperature, the SiO₂@CMP/glass plate was taken out, washed with ethanol (100 mL) three times, and dried in an oven at 50°C for 3 h. For the etching of silica spheres, the SiO₂@CMP/glass plate was added to 10% HF aqueous solution (50 mL) in a square dish. The separated glass plate was removed after ~1 min. After the resultant MA-CMP-F was further treated with the HF solution for additional 2 h, it was washed with ethanol (100 mL) three times. The MA-CMP-F was transferred to polytetrafluoroethylene film (PTFE, thickness of 0.1 mm, Sigma Aldrich Co.) and dried in an oven at 80°C for 1 h.

For the preparation of control CMP-F, the same synthetic procedures as those of MA-CMP-F were applied except using TLC plate (Silica gel 60 F₂₅₄ 25 aluminium sheets, Merck Milipore) with size of 6 cm × 2.5 cm instead of the glass plate with assembled silica spheres. In addition, ~ a half amount (24 ~ 28 μmol) of the 1,1,2,2-tetra(4-bromophenyl)ethane and 1,1,2,2-tetra(4-ethynylphenyl)ethane were used. Based on the experimental characterization of thickness of control CMP-F by SEM analysis, the CMP-F with a thickness of 2.3 μm was used for the sensing tests. The other synthetic procedures for CMP-F were the same as those for MA-CMP-F.

Synthetic procedure for MA-CMP-F bearing porphyrins in Figure 5³

Tetra(4-ethynylphenyl)porphyrin and tetra(4-ethynylphenyl) Cr-Cl porphyrin were prepared by the synthetic procedures in the literature.^{4,5} The glass plate with assembled silica spheres (the plate was cut to the size of 6 cm × 2.5 cm) was added to a Rodaviss glassware (100 mL). After (PPh₃)₂PdCl₂ (1.3 mg, 1.9 μmol), CuI (0.3 mg, 1.6 μmol), and triethylamine (TEA, 10 mL) were added to a 10 mL vial, the solution was sonicated for 1 min and then, added to the Rodaviss glassware. After toluene (40 mL) was added to the Rodaviss glassware, the mixture was stirred for 2 h. Tetra(4-ethynylphenyl)porphyrin (25 mg, 35 μmol) and 1,4-diiodobenzene (23 mg, 70 μmol) were dissolved in THF (5 mL). After the solution was added to the Rodaviss glassware, the mixture was stirred at 600 rpm for 10 min and heated at 90°C overnight *without stirring*. After being cooled to room temperature, the SiO₂@CMP/glass plate was taken out, washed with ethanol (100 mL) three times, and dried in an oven at 50°C for 3 h. For the etching of silica spheres, the SiO₂@CMP/glass plate was added to 7.5% HF aqueous solution (50 mL) in a square dish. The separated glass plate was removed after ~1 min. After the

resultant MA-CMP-F was further treated with the HF solution for additional 2 h, it was washed with a mixture of methanol and water (100 mL) three times. The MA-CMP-F containing metal-free porphyrin was transferred to polytetrafluoroethylene film (PTFE, thickness of 0.1 mm, Sigma Aldrich Co.) and dried in an oven at 80°C for 1 h. For the preparation of MA-CMP-F containing Cr-F porphyrins, tetra(4-ethynylphenyl) Cr-Cl porphyrin (35 μ mol) was used instead of tetra(4-ethynylphenyl) porphyrin. During the silica etching by HF, the Cr-Cl species in porphyrins were converted to Cr-F species, as reported in the literature.⁵

Experimental procedure of sensing tests

The sensing tests were conducted using MA-CMP-F or CMP-F with a size of 0.5 cm \times 1 cm. The MA-CMP-F and CMP-F on the PTFE film were transferred to a slide glass plate and attached with a double side tape. DNT, 4NT, 2NT, 4CT, and T solution with concentrations of 0, 0.0025, 0.0050, 0.010, 0.15, 0.020, 0.050, 0.125, and 0.50 mM were prepared in ethanol. Each solution of 3 mL was used for the sensing tests. The emission intensity changes at 517 and 525 nm for MA-CMP-F and CMP-F, respectively, were measured using a JASCO FP-6200. Considering the conventional range of visible light, the excitation wavelength was fixed to 410 nm. After the MA-CMP-F and CMP-F on the glass plates were added to ethanol and left for 2 h until the system reached equilibrium with no changes of emission intensity, the solution was replaced with that with analytes. After leaving the system for 1 h, the changes of emission intensities were measured. K_{sv} values were measured by plotting I_0/I vs $[M]$; the Stern-Volmer plot ($I_0/I = K_{sv}[M] + 1$, I_0 : the original emission intensity, I : the intensity of emission in the presence of analytes, M : the concentration of substrates in water, $R^2 > 0.99$ for linear regression) Recycling tests were conducted using 0 mM and 0.50 mM solutions of 4NT alternatively. Before each sensing cycle for 4 NT, the retrieved MA-CMP-F was washed with excess ethanol three times.

Procedure for computational simulation (Figures S3-5)

In order to shed light on the emission quenching behaviors of MA-CMP-F by nitrotoluenes, we performed the density functional theory (DFT) calculations on the HOMO-LUMO energy levels of MA-CMP-F and substrates. The geometrical optimizations for model systems of MA-CMP-F (CMP-1, CMP-4 and CMP-P refer to Fig. S5 in the ESI for the definition), TNT, DNT, 4NT, 2NT, 4-chlorotoluene (4CT), toluene (T), and additional toluene derivatives having monosubstituent at para position were carried out within B3LYP/light-tier1 level of theory using FHI-aims code.⁶ The convergence criteria were set to 10^{-2} eV/Å except for the CMP-P case. For CMP-P, the PBE/light-tier1 level and 2×10^{-2} eV/Å of relaxation setting were used to conduct the periodic boundary condition (PBC) calculation with full relaxation for both atomic geometries and unit cell parameters, because computational costs for PBC calculations with hybrid functional are enormously expensive. Then, single point calculation at B3LYP/light-tier1 level was performed to estimate the HOMO and LUMO energy levels for CMP-P. It is noted that in a PBC calculation actually the HOMO and LUMO energy levels indicate the valence band maximum and conduction band minimum, respectively. The optimized unit

cell parameters of CMP-P were calculated to be $21.49 \text{ \AA} \times 16.29 \text{ \AA} \times 35.75 \text{ \AA}$. The vacuum space of about 30 \AA was added along the c-axis to avoid the interactions between 2-dimensional sheets. In addition, single point molar volume calculations at the optimized geometries for TNT, DNT, 4NP and 2NT were carried out to understand the size effect on the sensitivity of experimental sensing behavior using Gaussian 09 package.⁷

Theoretically, it is expected that the LUMO energy levels of MA-CMP-F are located around $-2.31 \sim -2.89 \text{ eV}$ which can possibly be modulated by the conjugation length of CMP moieties. The calculated relative LUMO energy levels of substrates indicate that the electron transfers from the excited MA-CMP-F to nitrotoluenes including TNT might be favorable to lead fluorescent quenching. On the other hand, the mismatch of LUMO energy levels 4CT and T prevents the induction of emission quenching of CMP materials, which is fully consistent with the experimental fluorescent sensing behavior. It is noteworthy that our DFT results indicate that MA-CMP-F can also be used for the detection of TNT compound. In the experimental results, the sensing efficiencies of MA-CMP-F towards nitrotoluenes were observed in the increasing order of $\text{DNT} < 2\text{NT} < 4\text{NT}$. This trend can be analyzed considering both the size and electronic effects of substrates. From the aspect of the diffusion process, we can speculate that smaller substrates (4NT and 2NT) would have higher sensing efficiencies than DNT. (Refer to Fig. S7 in the ESI for the calculated molar volume values and size parameters) In the case of 4NT and 2NT having similar molecular volumes, the calculated LUMO energy level of 4NT is rather lower than that of 2NT. Thus, the 4NT as photo-induced electron acceptor has a better quenching efficiency than 2NT.

Reference

1. W. Stöber, A. Fink and E. Bohn, *J. Colloid Inter. Sci.* 1968, **26**, 62-69.
2. Y. Xu, D. Chang, S. Feng, C. Zhang and J. -X. Jiang, *New J. Chem.* 2016, **40**, 9415-9423.
3. Y. J. Shin, *MS thesis*, Sungkyunkwan University, 2016.
4. Z. Wang, S. Yuan, A. Mason, B. Reprogle, D. -J. Liu and L. Yu, *Macromolecules* 2012, **45**, 7413-7419.
5. M. H. Kim, T. Song, U. R. Seo, J. U. Park, K. Cho, S. M. Lee, H. J. Kim, Y. -J. Ko, Y. K. Chung and S. U. Son, *J. Mater. Chem. A* 2017, **5**, 23612-23619.
6. V. Blum, R. Gehrke, F. Hanke, P. Havu, V. Havu, X. Ren, K. Reuter and M. Scheffler, *Comput. Phys. Commun.* 2009, **180**, 2175–2196.
7. M. J. Frisch, G. W. Trucks, H. B. Schlegel, G. E. Scuseria, M. A. Robb, J. R. Cheeseman, G. Scalmani, V. Barone, B. Mennucci, G. A. Petersson, H. Nakatsuji, M. Caricato, X. Li, H. P. Hratchian, A. F. Izmaylov, J. Blonino, G. Zheng, J. L. Sonnenberg, M. Hada, M. Ehara, K. Toyota, R. Fukuda, J.; Hasegawa, M. Ishida, T. Nakajima, Y. Honda, O. Kitao, H. Nakai, T. Vreven, Jr. J. A. Montgomery, J. E. Feralta, F. Ogliaro, M. Bearpark, J. J. Heyd, E. Brothers, K. N. Kudin, V. N. Staroverov, T. Keith, R. Kabayashi, J. Normand, K. Raghavachari, A. Rendell, J. C. Burant, S. S. Iyengar, J. Tomasi, M. Cossi, N. Rega, J. M. Millam, M. Klene, J. E. Knox, J. B. Corss, V. Bakken, C. Adamo, J. Jaramillo, R. Gomperts, R. E. Stratmann, O.

Yazyev, A. J. Austin, R. Cammi, C. Pomelli, J. W. Ochterski, R. L. Martin, K. Morokuma, V. G. Zakrzewski, G. A. Voth, P. Salvador, J. J. Dannenberg, S. Dapprich, A. D. Daniels, O. Farkas, J. B. Foresman, J. V. Ortiz, J. Ciosolowski and D. J. Fox, *Gaussian 09, Revision B.01*, Gaussian, Inc., Wallingford CT, 2010.

Fig. S1 A photograph and SEM images of the 400 nm silica spheres assembled on the glass plate.

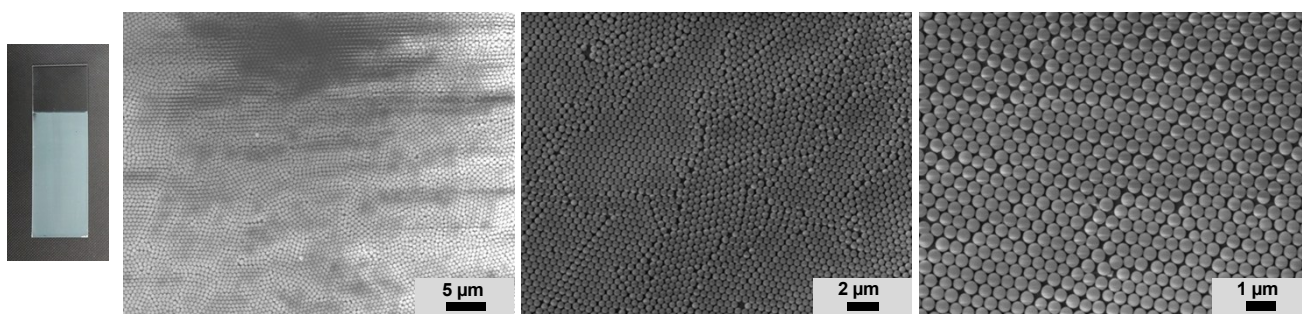
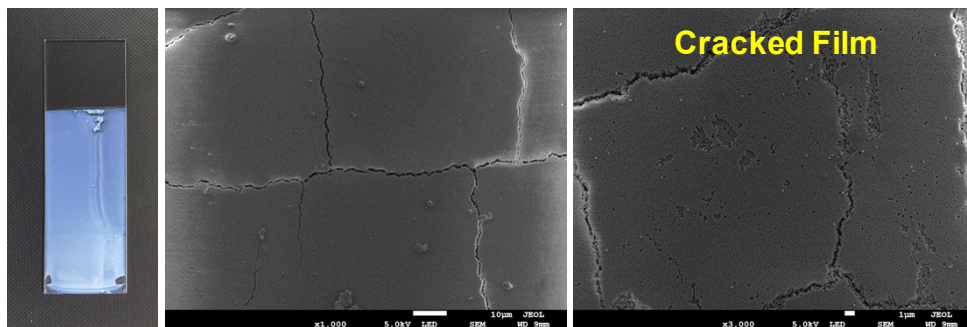


Fig. S2 Photographs and SEM images of 200 nm and 1.2 μm silica spheres assembled on the glass plate.

200 nm



1.2 μm

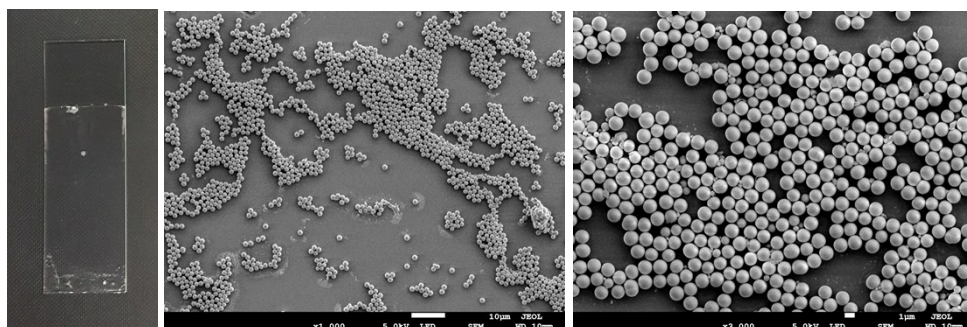


Fig. S3 Consideration of void space portion in MA-CMP-F induced by the 400 nm silica templates (supposing

the closest packing structure of hollow CMP spheres).

R = radius of silica spheres = 200 nm, a = edge distance of unit cell (nm)

$a = 2 \times 1.414 \times (R + 17.5) \text{ nm}$

Void space percent induced by silica templates

$= \{[\text{Inter sphere void space} + \text{hollow space of 4 hollow spheres}]/\text{unit cell volume}\} \times 100\%$

$= \{[\text{unit cell volume} - \text{volume of 4 hollow CMP spheres} + \text{volume of 4 hollow space}]/\text{unit cell volume}\} \times 100\%$

$= \{[a^3 - 4 \times (4/3) \times \pi (R+17.5)^3 + 4 \times (4/3) \times \pi R^3]/a^3\} \times 100\%$

$= \{[22.63(R+17.5)^3 - 16.76 (R+17.5)^3 + 16.76 R^3]/[22.63(R+17.5)^3]\} \times 100\%$

$= [0.2594 + 0.7406 R^3/(R+17.5)^3] \times 100 \% = 84\%$

Fig. S4 PXRD patterns of MA-CMP-F and CMP-F.

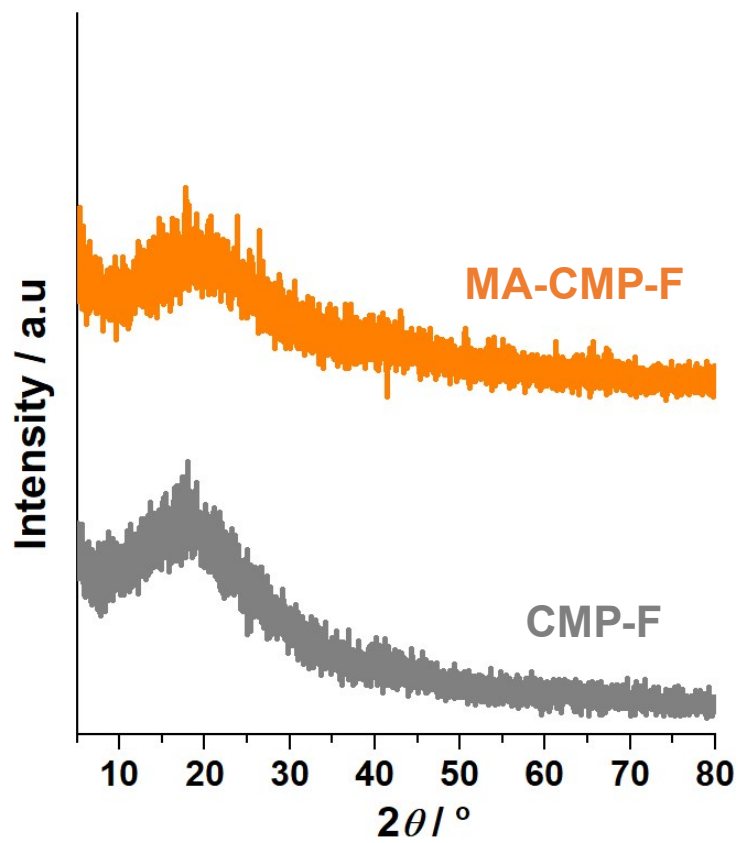


Fig. S5 Model systems (CMP-1, CMP-4, and CMP-P) of MA-CMP-F used for DFT simulation and their

optimized structures.

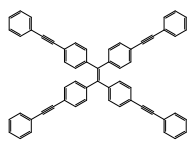

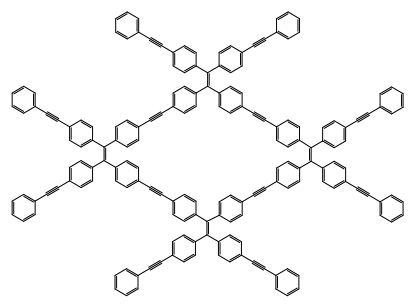
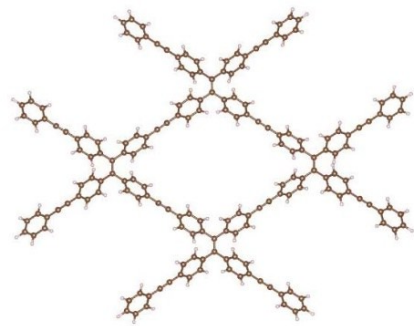
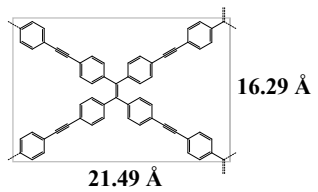
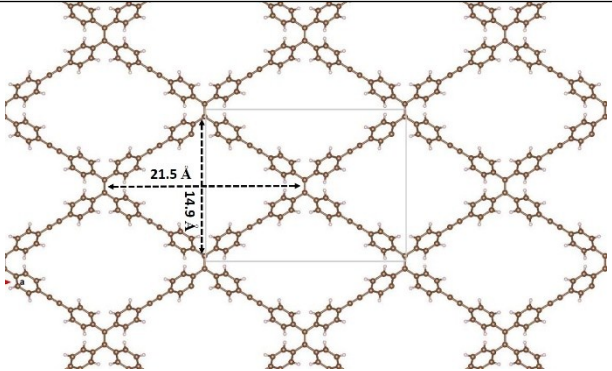
	Scheme	Optimized structures
CMP-1		
CMP-4		
CMP-P	<p>Unit cell</p> 	

Fig. S6 The cartesian coordinates (in Å) of optimized geometry for MA-CMP-F model systems.

CMP-1

Table with 4 columns: ID, Value 1, Value 2, Value 3. Contains 100 rows of numerical data.

CMP-4

Table with 4 columns: ID, Value 1, Value 2, Value 3. Contains 100 rows of numerical data.

Table with 4 columns: ID, Value 1, Value 2, Value 3. Contains 100 rows of numerical data.

Table with 4 columns: ID, Value 1, Value 2, Value 3. Contains 100 rows of numerical data.

C	50.71569330	23.60091301	23.87260647
C	50.27785344	21.29992503	25.37689105
H	52.16873933	21.71663551	26.28631534
C	49.55312927	22.86786722	23.68421291
C	50.88453703	24.49452766	23.28747942
H	49.31698582	21.70409556	24.43503356
H	50.10339614	20.40531723	25.95725290
H	48.81814665	23.18451072	22.95816718
C	48.12872263	20.94823333	24.24287652
C	47.11870038	20.30450780	24.07603089
C	45.93584845	19.54643881	23.87103709
C	44.98677660	19.93780778	22.91199478
C	45.68228529	18.38803579	24.62029559
C	43.83552892	19.19504900	22.71564108
H	45.16270597	20.82981670	22.32789517
C	44.53548070	17.64304058	24.4082334
H	46.39404247	18.08111994	25.37673227
C	43.59346137	18.02176236	23.44431432
H	43.11400862	19.52181989	21.97956142
H	44.36360010	16.75469841	25.0022622
C	22.53443059	31.68948206	24.68297952
C	21.63662762	32.27484351	24.82539398
H	11.86747013	23.18438818	21.54077951
C	41.00325814	31.68033194	21.53681382
C	11.86726416	9.93299265	24.77203087
C	41.01264971	1.45370727	24.79815006
H	41.91110186	0.87068668	24.94596659
C	22.55780378	1.40468964	21.59856281
C	51.66059570	9.92984758	21.48748983
H	52.56541486	9.35535818	21.34520943
C	51.66162849	23.19128175	24.80856181
H	52.56668793	23.76498797	24.95249303
H	41.90256543	32.26392672	21.39645813
H	10.96119574	23.75832244	21.40575515
H	10.96093971	9.36068228	24.91111180
H	21.66136683	0.81694860	21.45737502

CMP-P

C	10.63075739	8.70591649	19.58547846
C	10.62646535	7.33218841	19.58449560
C	9.37298037	6.53257770	19.52672885

C	9.18734058	5.47124813	20.43600276
C	8.35517687	6.78733431	18.58716284
C	8.01633472	4.73345199	20.45609384
C	7.18056724	6.04404104	18.58277872
C	6.97604475	5.01423826	19.52930880
C	11.87596792	6.52627842	19.64151282
C	12.06073785	5.47034557	18.72589742
C	12.89060212	6.77073994	20.58695745
C	13.23540810	4.72908816	18.70952155
C	14.06276279	6.02348210	20.59032846
C	14.26746095	5.00051274	19.63644675
C	11.88445746	9.50497164	19.52589878
C	12.07545304	10.56098997	20.44046187
C	12.89700757	9.25457253	18.57976609
C	13.25360260	11.29672069	20.45424745
C	14.07208745	9.99707622	18.7349108
C	14.28263307	11.02048122	19.52549946
C	9.28198596	9.51290226	18.45659002
C	9.19661861	10.56918763	19.36066729
C	8.6926871	9.26979107	20.59387949
C	8.02303607	11.31219767	18.71745487
C	7.19829476	10.01892325	20.60018626
C	6.99284935	11.04236880	19.64684879
C	5.78490362	11.78026679	19.61539652
C	4.74056990	12.41600829	19.56871390
C	5.76579086	4.28011334	19.56136664
C	4.72043563	3.64618728	19.60998839
C	15.47620306	4.26403539	19.60226822
C	16.522059215	3.62898557	19.54816146
C	15.49414380	11.75263704	19.55529381
C	16.53997768	12.38557780	19.60636791
C	17.72811456	2.89079223	19.51014950
C	18.76361300	3.15513873	20.43593310
C	17.92692320	1.86851452	18.5426068
C	19.83439651	2.40926556	20.41495182
C	19.09568950	1.11593503	18.55321052
C	20.11411097	1.35500229	19.49607958
C	3.51185063	2.90918003	19.63847171
C	2.47982687	3.18437611	18.17289386
C	3.30902052	1.87865214	20.58483490
C	1.30714297	2.43968713	18.72330065
C	2.13909797	1.12802209	20.57562381
C	1.12417012	1.37606927	19.63148886
C	3.53233182	13.15357550	19.54110960
C	3.33067129	14.18996925	18.60083487

C	2.49901398	12.87175358	20.46306755
C	2.15993010	14.93911036	18.61227645
C	1.32574812	13.61529315	20.45517266
C	1.14346168	14.68348337	19.55307967
C	17.74802565	13.12312550	19.64186836
C	17.95236631	14.14124920	20.60122174
C	18.77764034	12.86137741	18.79666879
C	19.12137651	14.89334418	20.59844568
C	19.94930560	13.60742514	18.72622621
C	20.13360542	14.65826746	19.64797582
C	21.38348345	15.46402686	19.59428849
C	21.36462671	0.55016831	19.54587578
H	9.97582260	5.24021398	21.15456864
H	8.48845393	7.58614323	17.85689613
H	7.87017360	3.93409747	21.17910348
H	6.40031398	6.25677835	17.85160532
H	11.27319248	5.24608858	18.00354636
H	12.75771401	7.56527714	21.32231389
H	13.37500343	3.92236850	17.97809512
H	14.84143597	6.22725695	21.32604707
H	11.29027787	10.78911042	21.16360553
H	12.76050114	8.45716108	17.84851571
H	13.39833960	12.09248680	21.18586713
H	14.84944372	9.78926696	17.83779134
H	9.98259754	10.79141772	18.00655907
H	8.50306005	8.47510779	21.32895883
H	7.88272344	12.10900595	17.98627140
H	6.42130645	9.81633601	21.33802973
H	18.62770927	3.94834109	21.17201655
H	17.14490253	1.66929167	17.82114208
H	20.72371580	2.62869107	21.13624243
H	19.22062082	0.23015326	17.81816373
H	2.61707411	3.98637383	17.98680532
H	4.08768169	1.67190378	21.31973669
H	0.51960520	2.66696512	18.00244281
H	2.00760975	0.2823309	21.30555630
H	4.11217223	14.40265722	17.87090568
H	2.63575154	12.06498793	21.18390525
H	2.03010078	15.74489247	17.88903815
H	0.53655607	13.38393509	21.17286664
H	17.17522436	14.33675815	21.34078771
H	18.63931797	12.06874680	17.97356402
H	19.25431797	15.68333010	21.33871159
H	20.73506814	13.39082153	18.00016368

Fig. S7 The calculated molar volumes (in cm^3/mol) and size parameters of nitrotoluene substrates (TNT, DNT,

4NP and 2NT) at B3LYP/6-31+G(d,p) level of theory with Gaussian 09 packages.

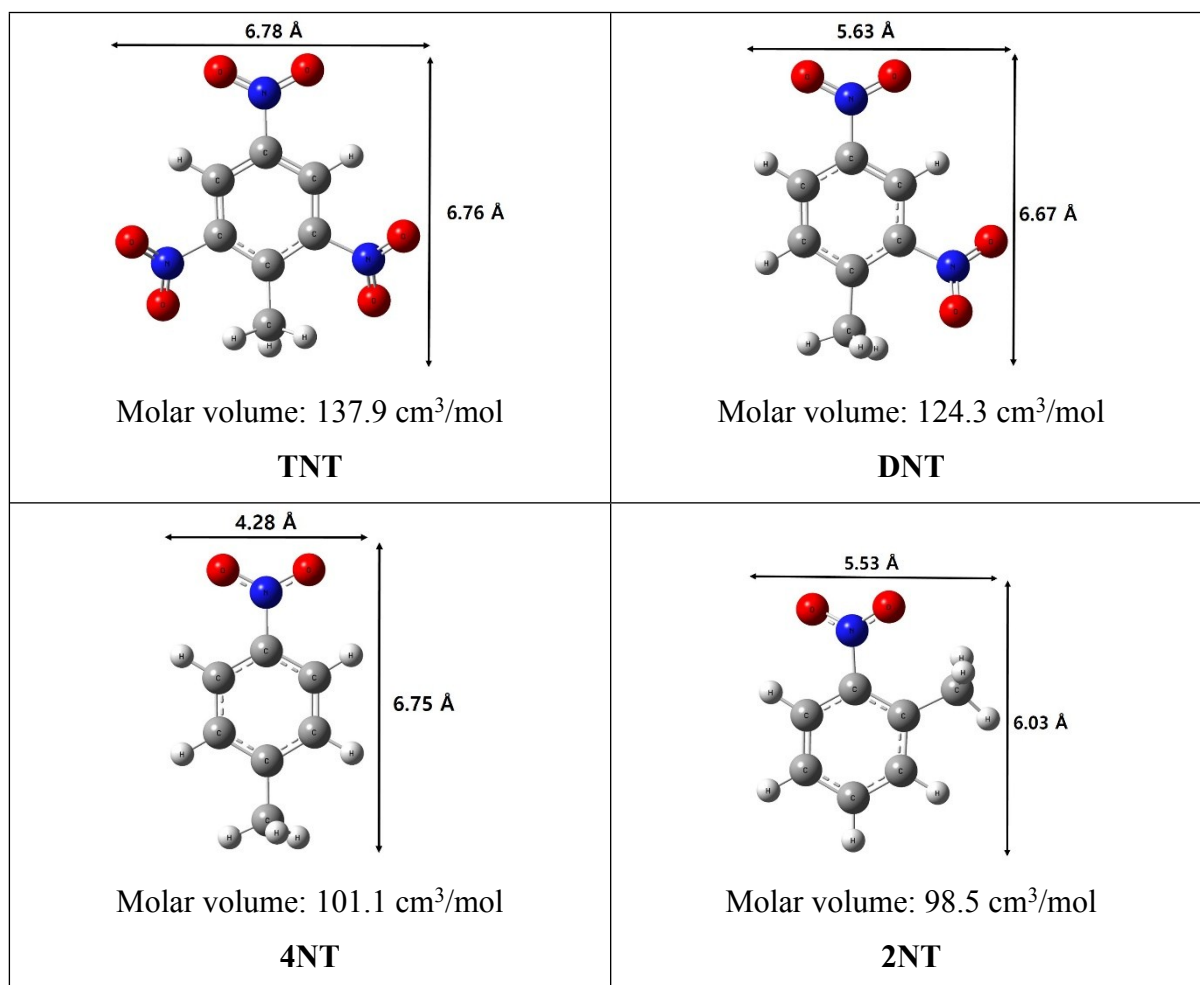


Fig. S8 The Stern-Volmer plots (I_0/I vs $[M]$) of the emission quenching of MA-CMP-F and CMP-F by 4NT,

2NT, and DNT.

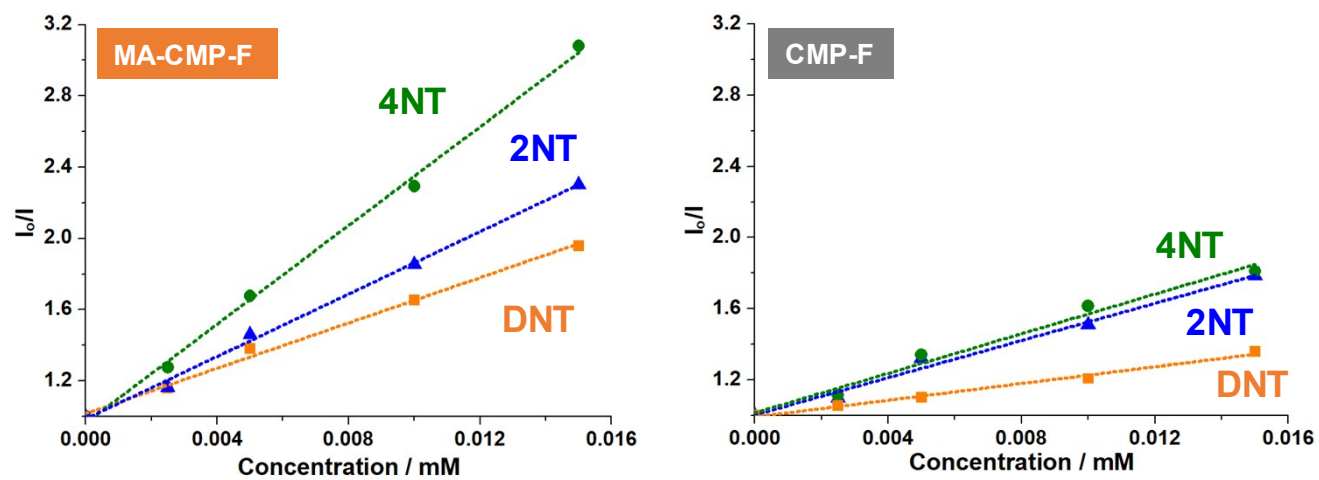


Fig. S9 Low magnification SEM image of MA-CMP-F recovered after the fifth recycle tests.

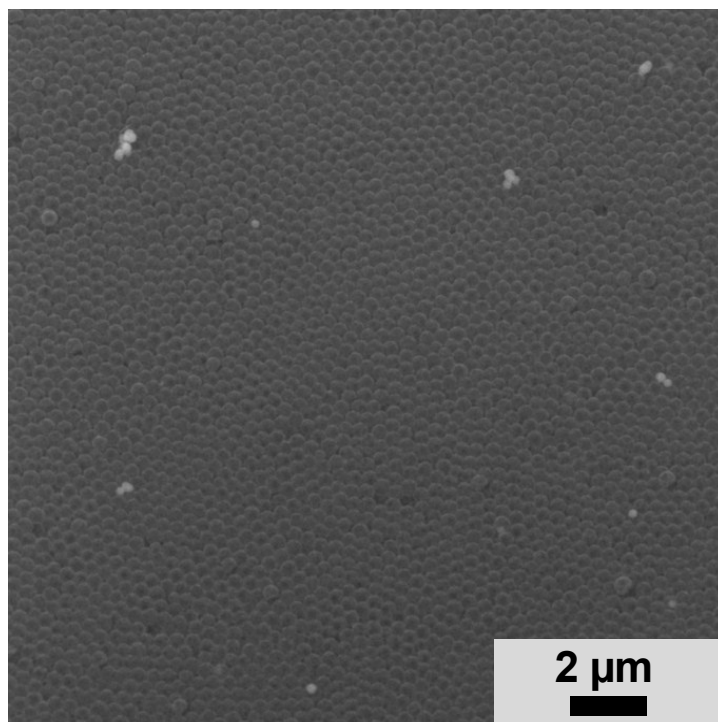


Fig. S10 Photographs of emission quenching of MA-CMP-F by 4NT.

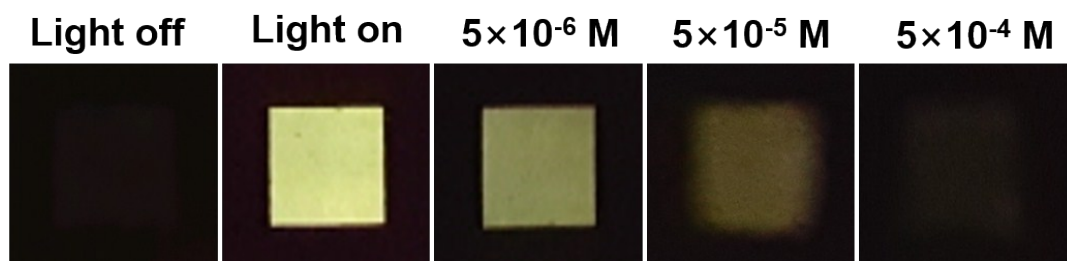
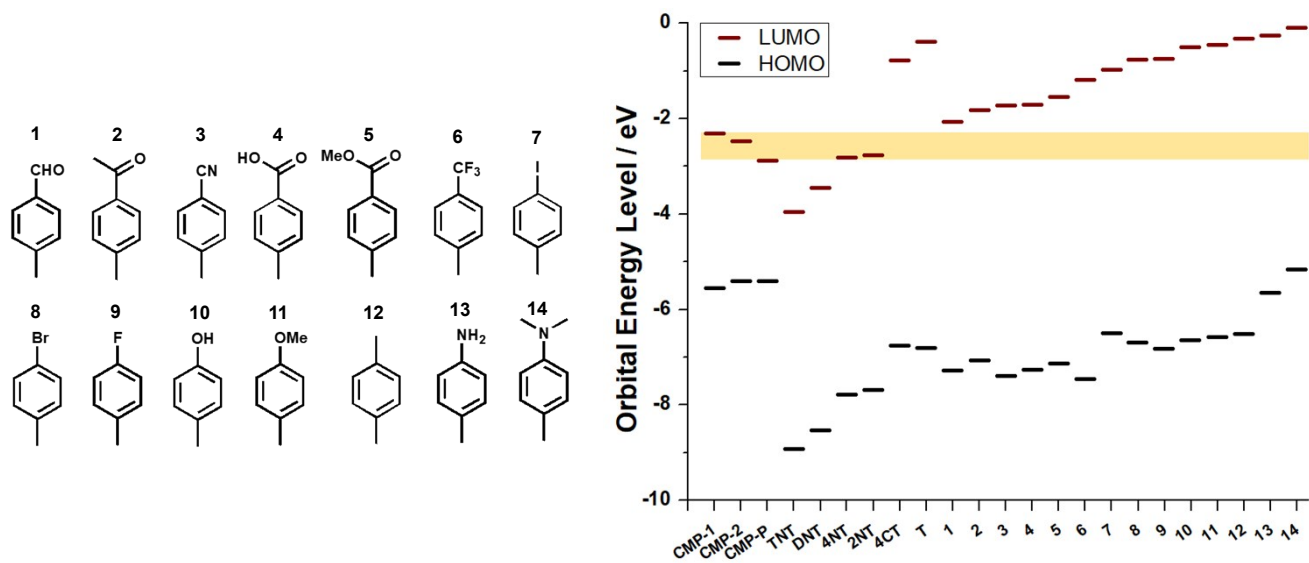


Fig. S11 The simulated HOMO and LUMO energy levels of additional toluene derivatives.



Entry	Systems	LUMO level (eV)	HOMO level (eV)	Entry	Systems	LUMO level (eV)	HOMO level (eV)
1	CMP-1	-2.31	-5.55	13	4	-1.71	-7.26
2	CMP-2	-2.47	-5.40	14	5	-1.54	-7.13
3	CMP-P	-2.89	-5.40	15	6	-1.18	-7.45
4	TNT	-3.96	-8.92	16	7	-0.98	-6.50
5	DNT	-3.44	-8.53	17	8	-0.77	-6.69
6	4NT	-2.82	-7.78	18	9	-0.74	-6.82
7	2NT	-2.77	-7.68	19	10	-0.50	-6.64
8	4CT	-0.78	-6.76	20	11	-0.46	-6.58
9	T	-0.39	-6.80	21	12	-0.32	-6.51
10	1	-2.07	-7.27	22	13	-0.26	-5.65
11	2	-1.82	-7.07	23	14	-0.09	-5.17
12	3	-1.72	-7.38				

Fig. S12 (a-c) The emission quenching behavior of MA-CMP-F in ethanol by O₂ and NO₂ in nitrogen (the S17

gases were bubbled into ethanol solution before measurements.) (d-e) The influence of O₂ and NO₂ in the emission quenching of MA-CMP-F in ethanol by 4NT (0.015 mM).

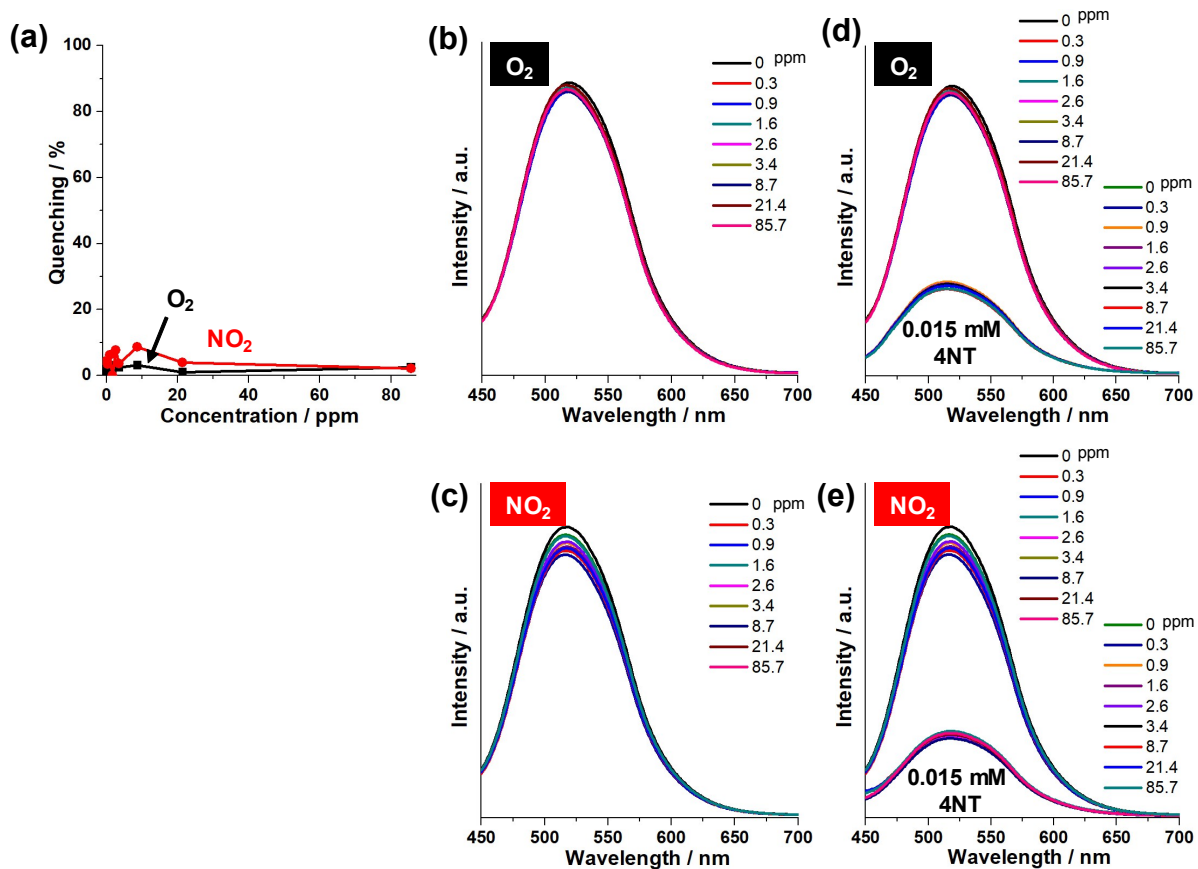


Fig. S13 (a) The emission quenching behavior of MA-CMP-F in ethanol by tetrabutylammonium perchlorate

and nitrate and (b) the Stern-Volmer plots.

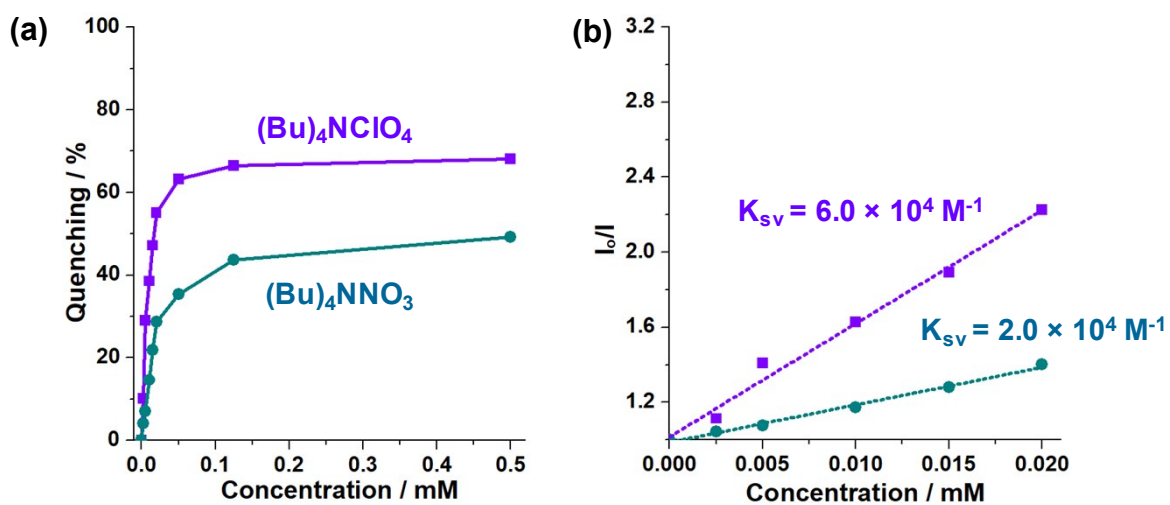


Fig. S14 (a) UV/vis absorption and (b) IR spectra of MA-CMP-F containing metal-free porphyrin and Cr-F
S19

porphyrin moieties. In UV/vis absorption spectra, the Q band peak of MA-CMP-F with metal-free porphyrins appeared at 655 nm (indicated by asterisk), confirming the metal-free porphyrin species. In IR spectra, the vibration peak of MA-CMP-F with Cr-F porphyrins appeared at 1010 cm^{-1} , indicating the Cr-porphyrin species. For the synthetic details, refer to experimental procedures in the ESI.

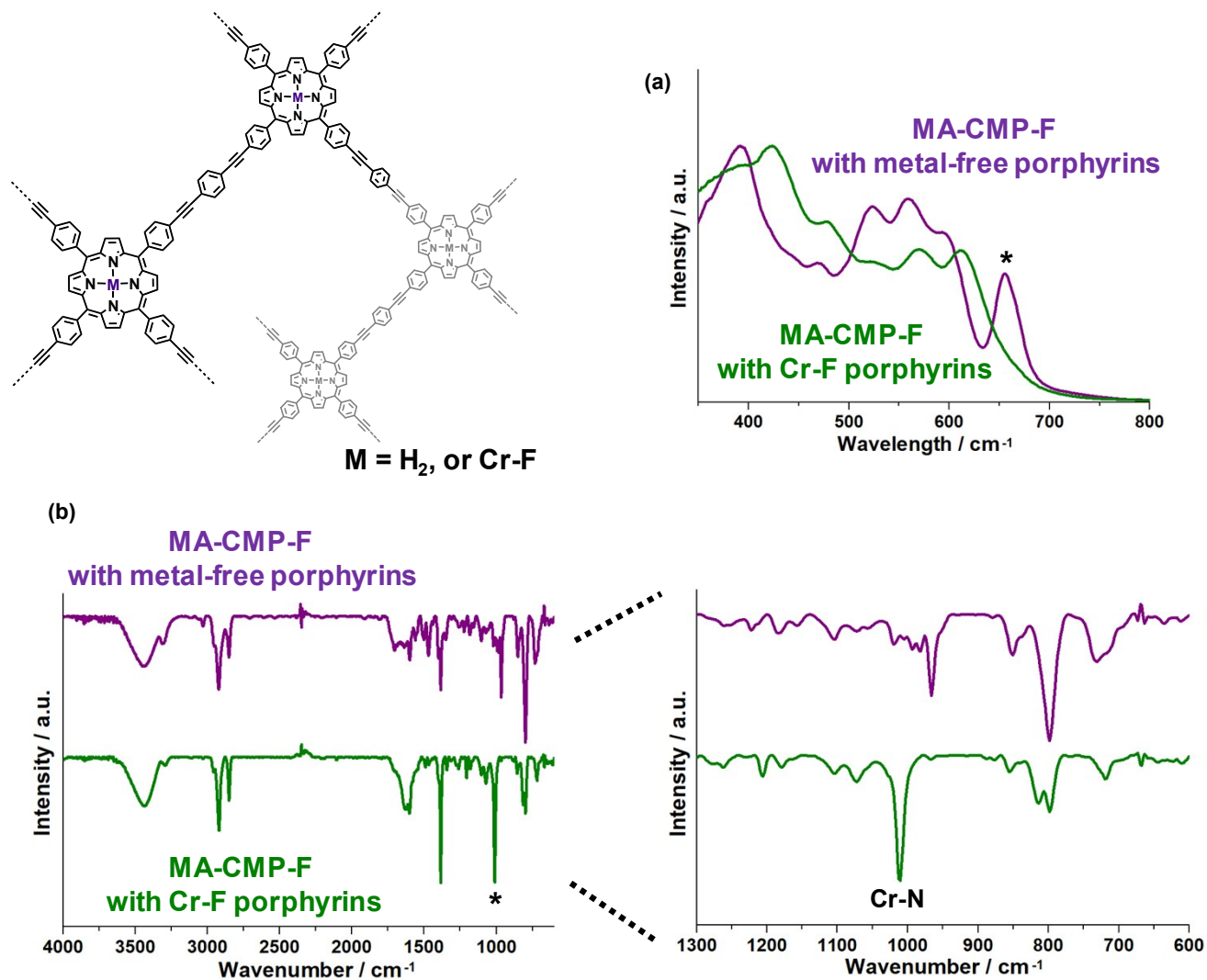


Table S1 Comparison of the sensing performance of MA-CMP-F with the results (best K_{sv} value) of emissive

CMP materials in the literature. TNP=2,4,6-trinitrophenol, TNB=1,3,6-trinitrobenzene, DNT=2,4-dinitrotoluene, TNT=2,4,6-trinitrotoluene, 2NP=2-nitrophenol, 4NT=4-nitrotoluene.

Entry	Materials	Substrate	Solvent	ex	K_{sv} (M^{-1})	ref
1	Microporous organic polymer with Troger base and TPEs	TNP	ethanol	380	26000	17
2	Nanoporous polymers with silsesquioxane and TPEs	-	chloroform	350	-	18
2	Dynamic covalent imine get	TNP	water	469	32220	19
3	Microporous polymer films with carbazole, thiophene, TPE	TNB	acetonitrile	340	67800	20
4	Nanofibrous PTBPE/PLA films	TNB	vapor	394, 380	-	21
5	Porous polymer films with carbazole and TPE	TNP	acetonitrile	331	64000	22
6	Porous polymer films with carbazole and TPE	DNT	acetonitrile	331	790	22
7	Conjugated porous polymer film	TNT	vapor	396	-	23
8	Conjugated microporous polymers with carbazole derivatives	DNT	acetonitrile	368	5900	31
9	Covalent organic polymer	TNP	THF	365	14500	32
10	Microporous organic polymers containing ethenylphenyl unit	TNP	THF: H ₂ O=9:1	365	-	33
11	Carbazole based conjugated microporous polymer	4NT	THF	380	4300	34
12	Porous hyperbranched conjugated polymer with triphenylamine	TNT	THF	353	1380	35
13	Sn-porphyrin network film	TNP	water	422	24000	36
14	Covalent organic polymer	TNT	methanol	365	2271	37
15	Highly cross-linked polymer with curcumins	TNP	methanol	372	15200	38
16	Hollow microporous organic network	TNP	THF:H ₂ O=1:2	440	15000	39
17	Conjugated porous polymer with carbazole and triphenylamine	2NP	dioxane	510	61200	40
18	Conjugated microporous polymers with fluorescein	TNP	THF	500	2080	41
19	MA-CMP-F	4NT	ethanol	410	138600	This work